sciendo
Polish Journal of Medical Physics and Engineering
The Journal of Polish Society of Medical Physics
ISSN 1898-0309, doi: 10.2478/pjmpe-2024-0017
September 2024
Vol 30, Issue 3

Scientific Paper

Monte Carlo dosimetry for BEBIG Cobalt-60 brachytherapy source with gynecological applicator in the presence of inhomogeneities

Farhad MORADI [1,ACD], Siti Fairus Abdul SANI [2,CE,*], Azman MAHYUDDIN [2,BCD], Ngie Min UNG [3,CE], David Andrew BRADLEY [4,5,AF], Kholoud ALMUGREN [6,CE], Hairul Azhar Abdul RASHID [1,AF,*]

[1]*Faculty of Engineering, Multimedia University, Jalan Multimedia, 63100, Cyberjaya, Malaysia*
[2]*Department of Physics, University of Malaya, Kuala Lumpur, Malaysia*
[3]*Clinical Oncology Unit, Faculty of Medicine, University of Malaya, 50603 Kuala Lumpur, Malaysia*
[4]*Applied Physics and Radiation Technologies Group, CCDCU, Sunway University, 46150 PJ, Malaysia*
[5]*Department of Physics, University of Surrey, Guildford, UK*
[6]*Department of Physics, Princess Nourah Bint Abdulrahman University, Riyadh, Saudi Arabia*
[*]*Corresponding authors: Dr. Siti Fairus Abdul Sani: s.fairus@um.edu.my, Prof. Hairul Azhar Abdul Rashid: hairul@mmu.edu.my*

(received 24 March 2024; revised 25 April 2024; accepted 27 June 2024)

Abstract

Introduction: High-dose-rate (HDR) ^{60}Co brachytherapy necessitates accurate dose calculations to minimize normal tissue toxicity and late malignancy risks. Conventionally, the American Association of Physicists in Medicine (AAPM) Task Group 43 (TG-43) formalism, utilizing table-based dose superposition, has been employed for dose calculations, overlooking tissue inhomogeneity effects.

Material and methods: This study focuses on characterizing the high-dose-rate BEBIG ^{60}Co brachytherapy source, in combination with a gynecological applicator, using Monte Carlo simulations. The investigation is based on the model of the modified BEBIG ^{60}Co source (Co0.A86) implemented at the University of Malaya Medical Center. Dosimetric properties are evaluated according to AAPM TG-43 formalism, with validation against existing published data.

Results: Our investigation presents comprehensive MC dosimetric properties of the high-dose-rate BEBIG ^{60}Co brachytherapy source, highlighting its accuracy in dose calculations compared to established data. The study also examined the impact of the applicator on depth dose calculations within a Krieger phantom and explored the influence of various tissue inhomogeneities on the depth dose.

Conclusions: Our findings revealed that the applicator had a relatively minimal effect on the delivered dose, with only marginal differences observed. Furthermore, we investigated the depth doses along the central axis of the applicator, within a segment characterized by various tissue inhomogeneities where dose differences of up to 12% were observed, with the lowest and highest doses recorded within bone and adipose tissues, respectively. This study underscores the valuable role of MC simulations in estimating doses at locations where physical measurements are unfeasible, such as the intra-uterine tube surface, as well as in scenarios featuring tissue inhomogeneities.

Keywords: brachytherapy; Monte Carlo simulation; dosimetry; HDR; BEBIG; ^{60}Co.

Introduction

Cancer treatment, particularly through radiation therapy, hinges on the precise delivery of therapeutic doses to cancerous tissues while minimizing damage to surrounding healthy structures. One established approach in radiation therapy is external beam techniques, well-suited for treating larger tumors. While external beam radiotherapy is typically considered less invasive and requires less labor, brachytherapy offers potential benefits, including shorter treatment durations and the ability to deliver high doses of radiation directly to the tumor site with steep dose gradients, potentially leading to better sparing of surrounding healthy tissues. Additionally, brachytherapy allows for tailored dose distributions and may be particularly advantageous for certain tumor locations or anatomical situations. For external beam radiotherapy, the International Commission on Radiation Units Measurements (ICRU) Report No. 50[1] has set forth the ideal target range for cancerous tissue to receive radiation doses, stipulating that they should fall within the range of 95% to 107% of the prescribed dose. Instead, for brachytherapy specific dose prescriptions and recommendations are typically outlined in

Authors' contribution:
A – Research concept and design, B – Collection and/or assembly of data, C – Data analysis and interpretation, D – Writing the article, E – Critical revision of the article, F – Final approval of the article.

clinical guidelines and consensus statements. These guidelines provide evidence-based recommendations tailored to specific cancer types and treatment modalities. Achieving the required level of precision is a challenging task, particularly when treating tumors that are situated in areas where radiation distribution can become highly inhomogeneous.

Various cancer types, including breast, prostate, lung, and esophageal cancers, have benefited from brachytherapy approaches. Nevertheless, the development of high-dose rate (HDR) brachytherapy marked a pivotal advancement, aimed at addressing limitations previously associated with low-dose-rate (LDR) brachytherapy, a method commonly employed for the treatment of cervical carcinoma.[2] Brachytherapy, and specifically high-dose rate (HDR) brachytherapy, offers unique advantages. Unlike low-dose-rate (LDR) brachytherapy, HDR brachytherapy is characterized by a rapid dose fall-off with distance from the radiation source. This feature leads to a significant increase in the radiation dose near the source, while simultaneously reducing the risk of radiation toxicity to adjacent healthy tissues.

While HDR brachytherapy stands as a widely accepted and practiced approach across the globe, it's important to note that its effectiveness can be influenced by the choice of isotope sources. In this context, isotopes such as ^{192}Ir and ^{60}Co are commonly employed. To illustrate, a study by Richter et al.[3] highlighted the physical properties of ^{60}Co and ^{192}Ir HDR sources. It demonstrated that within a specific proximity (e.g., within 22 cm from the source), the integral dose fall-off varies between these sources. Moreover, a key advantage of ^{60}Co over ^{192}Ir is its considerably longer half-life of 5.27 years. This extended half-life translates to a reduction of equipment downtime and offers practical and economic benefits.[4]

However, despite the well-established advantages of HDR brachytherapy, there remains a notable gap in research regarding a highly relevant aspect in this field - the effect of tissue inhomogeneities on the radiation dose distribution in close proximity to the brachytherapy applicator. The gynecological area, where brachytherapy is frequently employed, may exhibit variations in tissue density and composition or interfraction variations, potentially introducing inhomogeneities that influence dose delivery.[5-8] Addressing this concern and understanding its implications are important for optimizing cancer treatment.

Given the potential for anatomical variations and dynamic changes within the gynecological region and to explore this critical aspect, this research employs Monte Carlo (MC) simulation, which is known as a reliable and robust approach for dosimetric studies in both external beam radiotherapy and brachytherapy scenarios, particularly when measurements are costly or labor-intensive.[9-12] While characterizing established ^{60}Co HDR sources has been undertaken in prior studies,[4,13,14] this work endeavors to extend the knowledge base by modeling the ^{60}Co source and the gynecological applicator introduced by Eckert & Ziegler BEBIG GmbH company (Berlin, Germany). The primary objective is to evaluate the influence of the applicator on depth dose distributions in a standard phantom (Krieger phantom) and to scrutinize the effect of various tissue inhomogeneities in close proximity to the applicator. These critical investigations become increasingly pertinent in cases where physical measurements are challenging or virtually impossible, necessitating advanced simulation techniques. Following this introduction, we will detail the dose calculation formalism, elucidate the validation of MC simulations using the MCNPX code, and present the simulation results within the phantom.

Materials and methods

General formalism for 2D dose calculations

For brachytherapy sources that are cylindrically symmetric, the dose distribution can be considered two-dimensional and therefore be described in terms of a polar coordinate system with its origin at the source center as schematically shown in **Figure 1**.

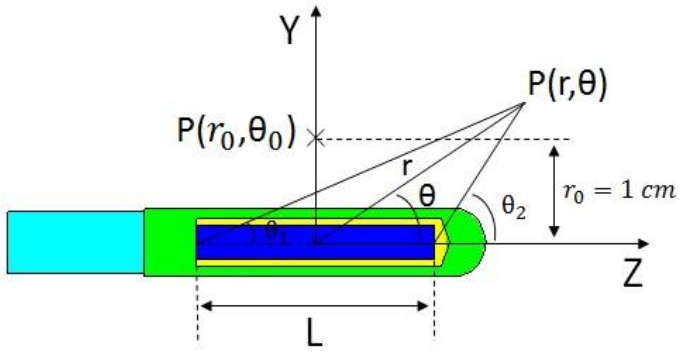

Figure 1. Coordinate system used for dosimetry calculations in this work (L = 0.35 cm) as suggested by AAPM TG-43[15]

Where *r* is the distance of the point of interest from the center of the source and θ is the angle with respect to the axis of the source cylinder. The general equation from AAPM protocol[15] for 2D dose calculation is

$$\dot{D}(r,\theta) = S_k \cdot \Lambda \cdot \frac{G_L(r,\theta)}{G_L(r_0,\theta_0)} \cdot g_L(r) \cdot F(r,\theta) \quad \text{Eq. 1}$$

In which, S_K and Λ are Air-kerma strength and dose-rate constant in water. $G_L(r,\theta)$, $g_L(r)$ and $F(r,\theta)$ represent the geometry function, the radial dose function and the 2D anisotropy function respectively.

As defined, the dose-rate constant in water is calculated by division of dose rate at the reference position, $P(r_0,\theta_0)$ to S_k.

$$\Lambda = \frac{\dot{D}(r_0,\theta_0)}{S_k} \quad \text{Eq. 2}$$

And the radial dose function, $g_L(r)$, is defined by **Equation 3**.

$$g_L(r) = \frac{\dot{D}(r,\theta_0)}{\dot{D}(r_0,\theta_0)} \cdot \frac{G_L(r_0,\theta_0)}{G_L(r,\theta_0)} \quad \text{Eq. 3}$$

In this study, the calculation of two primary parameters, namely, the dose-rate constant and radial dose function, as defined in the revised AAPM protocol for brachytherapy dose calculations[15], is performed for the purpose of validation against published data. Details of the calculation of other parameters are not presented here, as they are available in the mentioned protocol.

Monte Carlo simulations

The modeling of the BEBIG ^{60}Co HDR brachytherapy source type Co0.A86-1 was conducted using the MCNPX code (version 2.6) with the precise geometry provided by the manufacturer, as illustrated in **Figure 2**. Compositions and densities of all materials simulated in this step are listed in **Table 1**. The components that were modeled included the cylindrical active source (0.5 mm diameter, 3.5 mm length) made of ^{60}Co, situated within air, and enclosed by a 0.15 mm thick capsule made of stainless steel (316L) that was connected to a cable. Every point in the source was assumed to emit two ^{60}Co gamma lines of 1.1732 1.3325 MeV isotropically. Simulations were run in photon electron transport mode, and the air-kerma was computed at a 100 cm distance from the source center on the transverse axis within a ring-shaped cell with a 2 cm thickness and 1 cm height, similar to the method employed in a previous report[4].

To obtain dose distribution, the ^{60}Co source model was positioned at the center of a spherical water phantom with 50 cm radius that could be assumed as an infinite medium in this case. The dose was calculated using ring shape dosimeters with 0.5 mm thickness and 0.5 mm height, concentric to the central axis of the source. Various radial and longitudinal ring dosimeters positioned at distances ranging from 0.25 cm to 14 cm were considered to reproduce dose distributions reported in the work of Granero et al.[13] for the same source, Co0.A86-1. A sufficient number of histories were run to calculate the air-kerma and the radial dose function with an obtained uncertainty of better than 1% comparable to that documented in other reports. This was on the scale of 10^6 for air-kerma calculation and up to 2×10^9 for dose calculations. Energy cutoff for both photons and electrons were set to 0.01 MeV[16], while the effect of using the lower energy cut off equal to 0.001 MeV was also examined with almost negligible effect on radial dose function and depth doses observed.

In the second series of simulations, gynecological applicator constructed from stainless steel with the thickness of 0.75 mm along its length and 3 mm at the tip was modeled using the manufacturer's provided information. For depth dose calculations, the source and applicator were positioned within a PMMA phantom with the same specifications as the afterloading calibration phantom, commonly referred to as the Krieger phantom. This cylindrical phantom features dimensions of 20 cm in diameter and 12 cm in height, and is composed of polymethylmethacrylate with a density of 1.19 g/cm^3. It is specifically designed for the calibration and characterization of afterloading HDR brachytherapy sources.

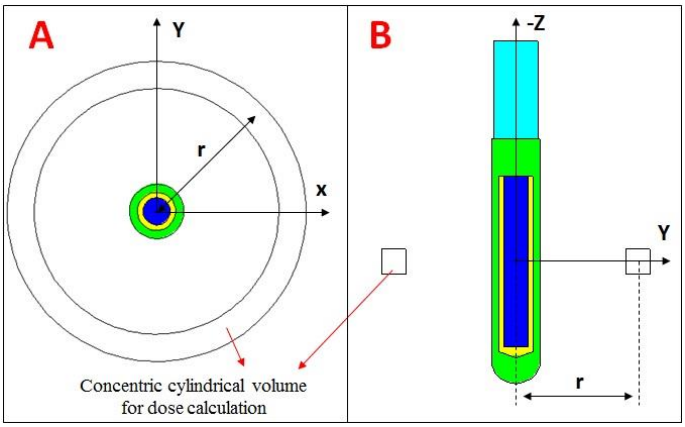

Figure 2. A) Cross-sectional view and B) Front view of the MCNPX simulated HDR BEBIG ^{60}Co brachytherapy source for calculation of the radial dose function

Table 1. Material compositions used in the MC simulations in this work in terms of weight percentage

Element	Air	Water	Stainless steel capsule	Steel cable	Cobalt
H	—	11.19	—	—	—
C	0.0124	—	0.03	0.03	—
N	75.527	—	—	—	—
O	23.178	88.81	—	—	—
Si	—	—	1	1	—
P	—	—	0.045	0.045	—
S	—	—	0.03	0.03	—
Ar	1.2826	—	—	—	—
Cr	—	—	17	17	—
Mn	—	—	2	2	—
Fe	—	—	65.395	65.395	—
Co	—	—	—	—	100
Ni	—	—	12	12	—
Mo	—	—	2.5	2.5	—
Density (g/cm^3)	0.0012	—	8.03	4.81	8.9

Figure 3a and **3b** show the schematic of the simulation setup to obtain depth dose on the central (longitudinal) axis of the source without and with the presence of the applicator. Dosimeter cells were considered as cylinders with 0.5 mm diameter and 0.5 mm height on the central axis located at distances from 0.5 to 10 mm away from the applicator's tip. To investigate the effect of tissue inhomogeneities, various materials including soft tissue, adipose, muscle, bone and water with compositions adopted from the ICRU Report 44[17] in the form of a cubic segment with dimensions 20×20×3 mm^3 were introduced within the PMMA phantom from 2.5 to 5.5 mm distance from the applicator's tip. **Figure 3c** demonstrates the schematic of the simulated setup with tissue inhomogeneity added to the phantom.

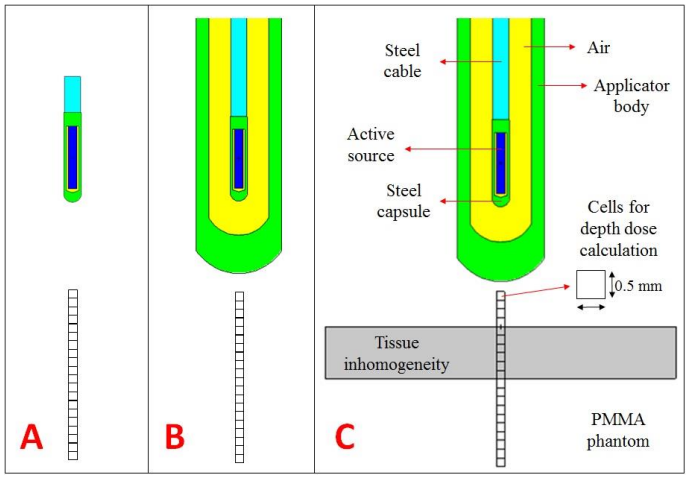

Figure 3. Simulations setup for depth dose calculation of BEBIG HDR Cobalt-60 source (a) without applicator and (b) with gynecological applicator (c) with applicator in the presence of inhomogeneities (figure not to scale)

Results and discussion

To validate the simulations, functions and parameters as per the TG-43U1 formalism were determined through MCNPX simulations, and these results were compared with the corresponding values reported by Granero et al.[13] for the same source. The air-kerma strength (S_K) was directly computed from the simulation outcomes in air, as detailed in 'Monte Carlo simulations' section. Subsequently, the dose-rate constant in water (Λ) was derived from the results of dose calculations in water using **Equation 2**. The calculated value was then compared to values obtained from other studies and the experimental data sourced from an institution currently utilizing this source (specifically, the Clinical Oncology Unit of the University of Malaya Medical Center-UMMC), as presented in **Table 2**.

Table 2. Comparison of the calculated dose-rate constant in water in this work with other references

Dose Rate Constant, Λ ($cGy\ h^{-1}\ U^{-1}$)	
This work	1.0893±0.0002
Experimental (UMMC)	1.087±0.012
[13]	1.087±0.0011
[4]	1.108±0.001
[16]	1.097

The radial dose function which is defined to characterize the dose fall-off on the source transverse-plane, was obtained as presented in **Table 3**. As it is observed the data are consistent with the results of Granero et al.[13] and except for the very close vicinity of the source (0.25 and 0.5 cm distance from the source's center), relative differences between the radial dose functions are less than 0.6 %, that fall within the uncertainties of the MC simulations.

Table 3. The radial dose function, g_L (r) of present work compared to that of ref. 13

Radius, r (cm)	Radial dose function, $g_L(r)$		Relative differences (%)
	This work	Granero et al.[13]	
0.25	0.9899	0.9633	2.96
0.5	1.0378	1.0498	1.14
0.75	1.0489	1.0483	0.05
1	1.0505	1.0483	0.21
1.5	1.0466	1.0446	0.19
2	1.0397	1.0360	0.37
2.5	1.0317	1.0300	0.17
3	1.0240	1.0213	0.26
4	1.0077	1.0040	0.36
5	0.9904	0.9864	0.41
6	0.9740	0.9700	0.41
8	0.9377	0.9337	0.43
10	0.9009	0.8959	0.55
14	0.8233	0.8186	0.58

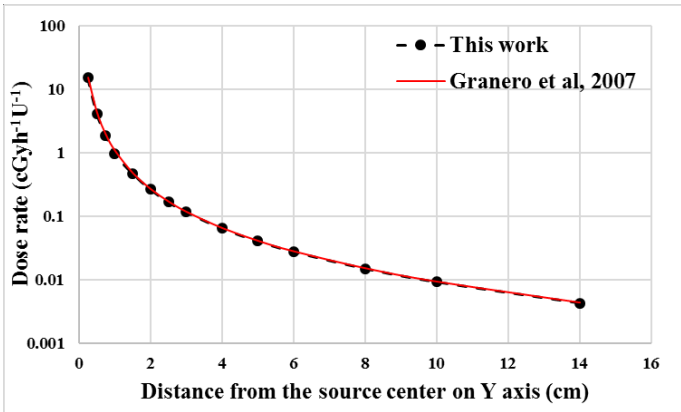

Figure 4. Dose rates per unit air-kerma strength calculated on transverse axis (Y) of the source in comparison to the published data

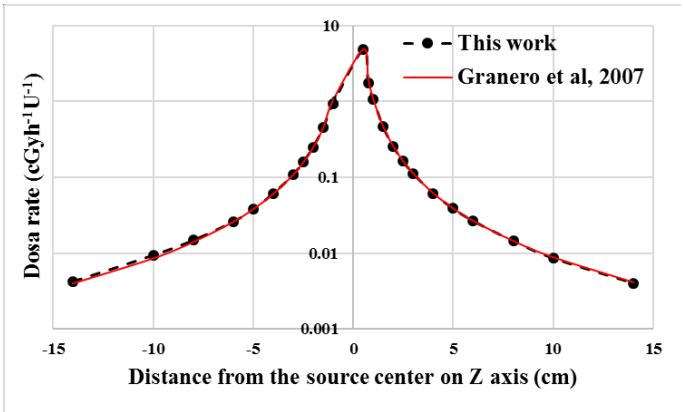

Figure 5. Dose rates per unit air-kerma strength calculated on central axis Z of the source in comparison to the published data

Calculated dose rates on transverse and central axes normalized to their maximum values are compared vs published data in **Figures 4** and **5**, respectively. It should be noted that the asymmetry of the dose rate curve in terms of distance from the source's center on the central axis stems from the asymmetric shape of the source on Z axis i.e., the existence of cable and steel capsule.

In order to have a detailed comparison of calculated values of dose rate in other positions, data obtained at various longitudinal distances on central axis (Z) including -10, -5, -1, -0.5, 0, 0.5, 1, 5 and 10 cm at various (radial) distances from the center on transverse axis (Y) ranged from 0 to 14 cm from our simulations were compared to the published data[13]. Results showed the differences as small as below 1 % in most cases while at very close distances to the source i.e., closer than 0.5 cm to the center on each of the axes, in a few points differences of up to 5.9 % are observed. Such differences and even higher values of up to 14% reported in other studies for points very close to the source, have been attributed to the possible impact of the length of the stainless-steel cable modeled in different simulations on the dose from scattered photons[16].

Subsequent to the validation of the MC simulations, depth doses within the Krieger phantom were computed for both the source, with and without the applicator, utilizing the configuration depicted in **Figures 3a** and **3b**. While the applicator enhances the effective positioning and delivery of the source to the tumor region, the results displayed in **Figure 6** reveal that its presence minimally reduces the dose at various depths without altering the dose rate falloff pattern. The resulting graph adheres to the inverse square law as distance increases, exhibiting a dose distribution pattern that aligns with prior reports.[18]

The simulation results for depth dose calculations, including the gynecological applicator and the presence of inhomogeneities, are depicted in **Figure 7**. For improved clarity, the inset within **Figure 7** provides a close-up view of the curves in the inhomogeneity region.

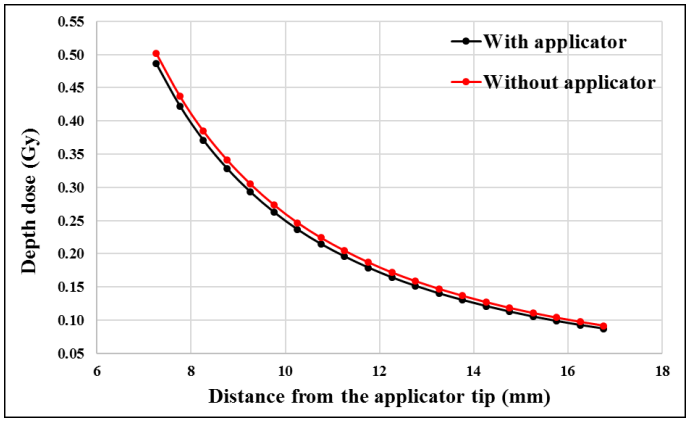

Figure 6. Depth dose in phantom with and without applicator

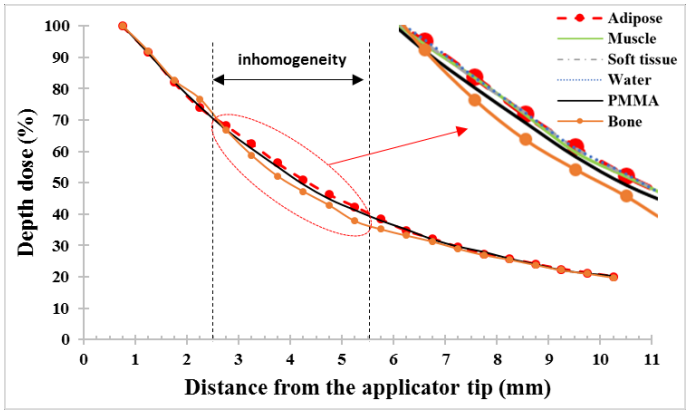

Figure 7. Comparison of depth doses by BEBIG 60Co source with gynecological applicator in PMMA phantom with various inhomogeneities

The influence of inhomogeneity presence becomes evident through variations in the depth dose, starting 0.5 mm (equivalent to one dosimeter cell) prior to the entrance surface of the inhomogeneity. Notably, the deposited dose in the region right before the bone exhibits a slight increase compared to the other curves, potentially attributed to the generation of scattered radiation by the bone. Within the region of inhomogeneity, relative differences of up to 12% were observed, with the dose

curve for PMMA positioned in the middle, while the doses in bone and adipose represented the lowest and highest values in the plot, respectively. Despite bone having a higher density compared to other tissues, the lower doses in bone can be attributed to its lower mass energy absorption coefficient of 2.745×10^{-2} cm^2/g, as opposed to, for instance, adipose with a value of 2.97×10^{-2} cm^2/g, at a photon energy of 1.25 MeV, which is equal to the average energy of ^{60}Co gamma rays. Depth doses in muscle, soft tissue, and water exhibited values nearly identical to those in adipose, with negligible differences. At the tissue slice's exit surface, the depth doses gradually converged, uniting at a point approximately 1.5 mm from the interface.

Conclusions

In this study, Monte Carlo simulations were conducted on the high dose rate BEBIG Cobalt-60 brachytherapy source model Co0.A86, employing the AAPM TG-43U1 updated formalism. Our findings revealed that the applicator had a relatively minimal effect on the delivered dose, with only marginal differences observed. Furthermore, we investigated the depth doses along the central axis of the applicator, within a segment characterized by various tissue inhomogeneities. Our results unveiled dose differences of up to 12%, with the lowest and highest doses recorded within bone and adipose tissues, respectively. This study underscores the valuable role of MC simulations in estimating doses at locations where physical measurements are unfeasible, such as the intra-uterine tube surface, as well as in scenarios featuring tissue inhomogeneities. By shedding light on the intricate interplay of radiation and varying tissue compositions, simulations contribute to the enhancement of brachytherapy treatment precision and safety.

References

1. Jones D. ICRU Report 50—Prescribing, Recording and Reporting Photon Beam Therapy. Medical Physics. 1994;21(6):833-834. https://doi.org/10.1118/1.597396
2. Nag S, Erickson B, Thomadsen B, et al. The American Brachytherapy Society recommendations for high-dose-rate brachytherapy for carcinoma of the cervix. Int J Radiat Oncol Biol Phys. 2000;48(1):201-211. https://doi.org/10.1016/S0360-3016(00)00497-1
3 Richter J, Baier K, Flentje M. Comparison of 60 Cobalt and 192 Iridium sources in high dose rate afterloading brachytherapy. Strahlenther Onkol. 2008;184(4):187-192. https://doi.org/10.1007/s00066-008-1684-y
4. Campos LT, de Almeida CEV. Monte Carlo dosimetry of the 60Co BEBIG high dose rate for brachytherapy. PLoS One. 2015;10(9). https://doi.org/10.1371/journal.pone.0139032
5. Grigsby PW, Georgiou A, Jeffrey FW, Perez CA. Anatomic variation of gynecologic brachytherapy prescription points. Int J Radiat Oncol Biol Phys. 1993;27(3):725-729. https://doi.org/10.1016/0360-3016(93)90402-H
6. Elhanafy OA, Das RK, Paliwal BR, Migahed MD, Sakr HA, Elleithy M. Anatomic variation of prescription points and treatment volume with fractionated high-dose rate gynecological brachytherapy. J Appl Clin Med Phys. 2002;3(1):1-5. https://doi.org/10.1120/jacmp.v3i1.2586
7. Co JL, Bojador MR, Mejia MBA, Ortin TTS, Ganzon DE. Interfraction variation and dosimetric changes in patients with cervical cancer treated with intracavitary brachytherapy. J Glob Oncol. 2017;4:1-7. https://doi.org/10.1200/JGO.2016.008557
8. Chernavsky NE, Morcos M, Wu P, Viswanathan AN, Siewerdsen JH. Technical assessment of a mobile CT scanner for image-guided brachytherapy. J Appl Clin Med Phys. 2019;20(10):187-200. https://doi.org/10.1002/acm2.12738
9. Moradi F, Ung NM, Khandaker MU, et al. Monte Carlo skin dose simulation in intraoperative radiotherapy of breast cancer using spherical applicators. Phys Med Biol. 2017;62(16):6550. https://doi.org/10.1088/1361-6560/aa7fe6
10 Setilo I, Oderinde OM, du Plessis FC. The effect of SSD, Field size, Energy and Detector type for Relative Output Factor measurement in small photon beams as compared with Monte Carlo simulation. Polish J Med Phys Eng. 2019;25(2):101-110. https://doi.org/10.2478/pjmpe-2019-0014
11. Fardi Z, Taherparvar P. A Monte Carlo investigation of the dose distribution for new I-125 low dose rate brachytherapy source in water and in different media. Polish J Med Phys Eng. 2019;25(1):15-22. https://doi.org/10.2478/pjmpe-2019-0003
12. Moradi F, Khandaker MU, Alrefae T, Ramazanian H, Bradley DA. Monte Carlo simulations and analysis of transmitted gamma ray spectra through various tissue phantoms. Appl Radiat Isot. 2019;146:120-126. https://doi.org/10.1016/j.apradiso.2019.01.031
13. Granero D, Perez-Calatayud J, Ballester F. Dosimetric study of a new Co-60 source used in brachytherapy. Med Phys. 2007;34(9):3485-3488. https://doi.org/10.1118/1.2759602

14. Badry H, Oufni L, Ouabi H, Hirayama H. Monte Carlo dose calculation for HDR brachytherapy source using EGS5 code. Radiat Phys Chem. 2018;150:76-81. https://doi.org/10.1016/j.radphyschem.2018.04.025
15. Rivard MJ, Coursey BM, DeWerd LA, et al. Update of AAPM Task Group No. 43 Report: A revised AAPM protocol for brachytherapy dose calculations. Med Phys. 2004;31(3):633-674. https://doi.org/10.1118/1.1646040
16. Selvam TP, Bhola S. EGSnrc-based dosimetric study of the BEBIG HDR brachytherapy sources. Med Phys. 2010;37(3):1365-1370. https://doi.org/10.1118/1.3326948
17. White DR, Booz J, Griffith RV, Spokas JJ, Wilson IJ. ICRU Report 44: tissue substitutes in radiation dosimetry and measurement. J Int Comm Rad Units Meas. 1989;23. https://doi.org/10.1093/jicru/os23.1.Report44
18. Jamalludin Z, Jong WL, Malik RA, Rosenfeld A, Ung NM. Characterization of MOSkin detector for in vivo dose verification during Cobalt-60 high dose-rate intracavitary brachytherapy. Phys Med. 2019;58:1-7. https://doi.org/10.1016/j.ejmp.2019.01.010